Journal Pre-proofs

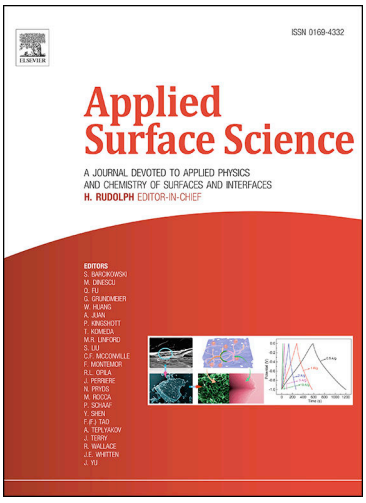


# Fast coating of hydrophobic upconversion nanoparticles by $NaIO_4$-induced polymerization of dopamine: Positively charged surfaces and *in situ* deposition of Au nanoparticles

Wei Zhang, Zhengfang Liao, Xiaoqi Meng, A. Erpuding Ai Niwaer, Hongyue Wang, Xinhua Li, Deming Liu, Fang Zuo

PII: S0169-4332(20)31578-6
DOI: https://doi.org/10.1016/j.apsusc.2020.146821
Reference: APSUSC 146821

To appear in: *Applied Surface Science*

Received Date: 12 February 2020
Revised Date: 22 May 2020
Accepted Date: 27 May 2020

Please cite this article as: W. Zhang, Z. Liao, X. Meng, A.E.A. Niwaer, H. Wang, X. Li, D. Liu, F. Zuo, Fast coating of hydrophobic upconversion nanoparticles by $NaIO_4$-induced polymerization of dopamine: Positively charged surfaces and *in situ* deposition of Au nanoparticles, *Applied Surface Science* (2020), doi: https://doi.org/10.1016/j.apsusc.2020.146821

# Fast coating of hydrophobic upconversion nanoparticles by $NaIO_4$-induced polymerization of dopamine: Positively charged surfaces and *in situ* deposition of Au nanoparticles

*Wei Zhang*[1], *Zhengfang Liao*[1], *Xiaoqi Meng*[1], *A Erpuding · Ai Niwaer*[1], *Hongyue Wang*[1], *Xinhua Li*[1], *Deming Liu*[2]*, *Fang Zuo*[1]*

1 College of Chemistry & Environment Protection Engineering, Southwest Minzu University, Chengdu 610041, China

2 State Key Laboratory of Luminescence and Applications, Changchun Institute of Optics, Fine Mechanics and Physics, Chinese Academy of Sciences, Changchun 130033, China

polymerzw@163.com; LiaoZfpolymer@163.com; polymermxq@163.com; polymerad@163.com; PolymerYue@163.com; lxh1905@126.com; liudeming@ciomp.ac.cn; polymerzf@swun.cn

**ABSTRACT:** In this work, hydrophobic upconversion nanoparticles (UCNPs) were transformed into hydrophilic NPs via the rapid oxidative polymerization of dopamine (DA) induced by $NaIO_4$ in a water-in-oil microemulsion system. The polydopamine (PDA)-coated UCNPs synthesized using $NaIO_4$ as the oxidant exhibited a positive charge (+26.4 mV) at pH 7.0. Those prepared using ambient $O_2$ as the oxidant had a negative charge (–15.4 mV). The difference in the composition between PDA-coated UCNPs using $NaIO_4$ (UCNPs@PDA-$NaIO_4$) and those using ambient $O_2$ (UCNPs@PDA-$O_2$) as oxidants was supported by the XPS and FTIR results. The difference in the surface charges may be due to variation in the composition, which probably attributed to the different oxidants used. A series of controlled experiments were carried out to infer the origination of the

positive charges of UCNPs@PDA-$NaIO_4$. Furthermore, Au nanoparticles (Au NPs) were deposited on UCNPs@PDA-$NaIO_4$ where PDA served as both the reductant and the stabilizer so that additional reagents and thermal treatments were not necessary. The effect of pH on the deposition of Au NPs was also studied. In addition, the load density of Au NPs on the surface of the PDA-coated UCNPs could be adjusted by changing the dosage of $HAuCl_4$, which could effectively enhance the upconversion luminescence (UCL) intensity. This work provides a method to regulate the surface charge of the PDA coating, and the nanocomposites with unique properties synthesized by this method may be employed in biological imaging, diagnostic analysis, and other biological fields.

**KEYWORDS:** Upconversion nanoparticles; Polydopamine; Positive charge; Au nanoparticles

# 1 Introduction

Upconversion nanoparticles (UCNPs) have been extensively investigated in biological applications because of their unique ability to absorb low-energy near-infrared light and emit high-energy visible light [1-5]. However, high-quality UCNPs are generally synthesized in organic solvents, and their surface is usually covered with oleic acid (OA) and/or oleylamine (OAm) ligands, rendering them hydrophobic [6-12]. Since UCNPs for biological applications require a high dispersibility and stability in aqueous media [6-12]. They also need suitable surface functional groups in order to facilitate the subsequent conjugation of biomolecules or probe molecules [6-12]. Thus, many different approaches to the surface functionalization and engineering of as-synthesized hydrophobic UCNPs have been developed [6-12]. The techniques may be divided into three main groups: ligand oxidation [7, 8], ligand exchange [9, 10], and encapsulation [11, 12].

Messersmith and coworkers pioneered the single-step formation of robust adherent polydopamine (PDA) coatings based on the mussel-inspired polymerization of dopamine (DA) at alkaline pHs on various substrates possessing both hydrophilic and hydrophobic surfaces [13]. PDA also received much attention in the surface modification of nanoparticles [14-16]. Recently, hydrophobic UCNPs were coated with PDA using a water-in-oil microemulsion method to obtain water-dispersible UCNPs@PDA core-shell nanocomposites [17-20]. The advantage of using PDA is that it can be easily functionalized with other molecules, mainly nucleophiles [13, 17]. Moreover, due to the presence of the catechol groups, PDA has a strong complexation ability with metallic cations and reduces them spontaneously *in situ* into metallic nanostructures [13, 21-27]. As a result, We conclude that PDA could serve as a versatile molecular platform to generate metallic nanoparticles (usually Ag and Au) with the desirable morphology and load density [21-27]. Thus, the functionalities of PDA have made these films of very interesting in the study of their applications [28, 29]. However, all the studies reported on PDA-coated hydrophobic UCNPs use dissolved $O_2$ as the oxidant, which is time-consuming, usually 24 h [17-20]. It has been reported that the use of oxidants stronger than dissolved $O_2$ allows for a faster deposition of PDA coatings [30-37]. Recently, some studies have indicated that the composition of PDA [32-37] and can affect the surface hydrophobicity [32, 33] and are influenced by the oxidant used. To date, only a few studies have been conducted to study the effect of oxidants on the surface charge of PDA coatings.

Here, OA-stabilized UCNPs were quickly coated with the PDA using the water-in-oil microemulsion method with $NaIO_4$ as the oxidant to obtain PDA-coated UCNPs (UCNPs@PDA-$NaIO_4$). The surface properties and compositions of UCNPs@PDA-$NaIO_4$ were characterized and compared with those obtained using the conventional slow PDA coating

(UCNPs@PDA-$O_2$) method. Furthermore, Au NPs were grown on the surface of UCNPs@PDA-$NaIO_4$ using the *in situ* reduction of $HAuCl_4$ by PDA. The influence of the load density of Au NPs on upconversion luminescence (UCL) was also studied. The fabrication procedure of Au NPs loaded UCNPs@PDA-$NaIO_4$ (UCNPs@PDA-$NaIO_4$/Au) is schematically illustrated in Scheme 1.

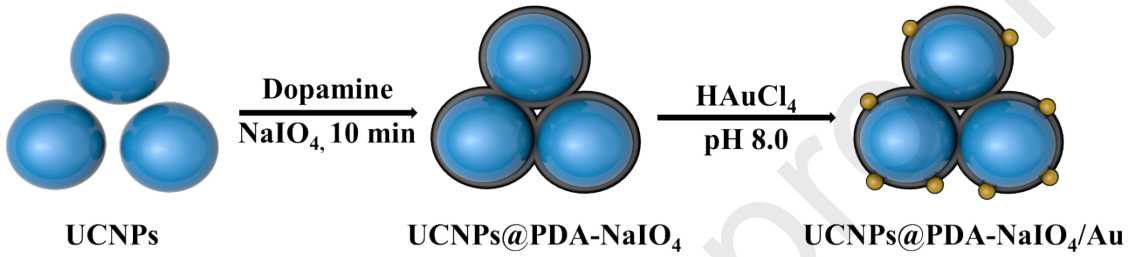


**Scheme 1.** Schematic representation of the formation of UCNPs@PDA-$NaIO_4$/Au NPs

# 2 Experimental

## 2.1 Materials

Yttrium chloride hexahydrate ($YCl_3 \cdot 6H_2O$, 99.99%), Ytterbium chloride hexahydrate ($YbCl_3 \cdot 6H_2O$, 99.99%) and Erbium chloride hexahydrate ($ErCl_3 \cdot 6H_2O$, 99.99%) were purchased from Shanghai Aladdin Biochemical Technology Co., Ltd. Oleic acid (OA, 90%) and 1-Octadecene (ODE, 90%) were supplied by Chengdu Shuobo Yanchuang Science and Technology Co., Ltd. Sodium hydroxide (NaOH, AR), Ammonium fluoride ($NH_4F$, AR), Ammonia solution (AR), Methanol ($CH_3OH$, AR), Ethanol ($C_2H_5OH$, AR) and Cyclohexane ($C_6H_{12}$, AR) were obtained from Chengdu Best Regent Co., Ltd. Chloroauric acid ($HAuCl_4$, ≥99.9%) and Dopamine hydrochloride (DA·HCl, 98%) were received from Beijing J&K Technology Co., Ltd. Polyoxyethylene (5)

nonylphenyl ether (Lgepal CO-520, branched, $M_w$ = 441, AR) was obtained from Shanghai Macklin Biochemical Technology Co., Ltd. Sodium periodate ($NaIO_4$, AR) was purchased from Tianjin Kemiou Chemical Reagent Co., Ltd. Unless otherwise noted, all materials were obtained from commercial supplies and used as received without further purification. Deionized water was used throughout.

## 2.2 Synthesis of hydrophobic UCNPs

The hydrophobic UCNPs were synthesized via a thermal decomposition method [38]. The details of the synthesis of 1 mmol $NaYF_4$:Yb/Er core nanoparticles in a typical procedure were described below. First, 0.76 mmol of $YCl_3 \cdot 6H_2O$, 0.2 mmol of $YbCl_3 \cdot 6H_2O$ and 0.04 mmol of $ErCl_3 \cdot 6H_2O$ were magnetically mixed with 6 mL of OA and 12 mL of ODE. The mixture was degassed under the $N_2$ flow, and then heated to 170 $^oC$ for 30 min to form a homogeneous clear solution and cooled to 50 $^oC$ while stirring. Afterwards, 10 mL of methanol solution containing NaOH (2.5 mmol) and $NH_4F$ (4.0 mmol) was added to the mixture solution and stirred for 30 min. After being stirred at 110 $^oC$ for 30 min to completely remove methanol and any residual water, the mixture solution was quickly heated to 305 $^oC$ and maintained for 90 min. After cooling down to room temperature, the products were precipitated by ethanol and washed with cyclohexane/ethanol/methanol several times. After that, the $NaYF_4$:Yb/Er core nanoparticles were re-dispersed in 10 mL cyclohexane, and then the inert $NaYF_4$ shell was deposited on the $NaYF_4$:Yb/Er core nanoparticles via a similar step. Finally, the obtained hydrophobic UCNPs were ready to be dispersed in cyclohexane prior to their further use.

## 2.3 Synthesis of UCNPs@PDA-oxidant ($NaIO_4$ or $O_2$)

The UCNPs@PDA-$NaIO_4$ were synthesized with a modified water-in-oil microemulsion

method [17]. Typically, 0.65 mL of Lgepal CO-520 was added in 10 mL of cyclohexane solution of hydrophobic UCNPs (1 mg/mL), and stirred vigorously for 20 min. Next, 0.075 mL of ammonia solution (25%) was carefully added into the solution, followed by ultrasonic treatment for 15 min and stirred gently for 30 min. After that, 0.05 mL of freshly prepared DA·HCl solution (25 wt%) was slowly injected into the solution. After stirring for 30 min, 0.05 mL of $NaIO_4$ solution (12.5 mg/mL) was injected into the above solution and stirred for another 10 min, 2 h, or 6 h. The products were precipitated by ethanol and washed with ethanol/water several times.

As a control, UCNPs@PDA-$O_2$ were prepared using the conventional slow strategy, i.e., reacted for 24 h after adding DA·HCl solution, in order to form a PDA coating.

## 2.4 Synthesis of UCNPs@PDA-$NaIO_4$/Au

In brief, $x$ ($x$ = 0.05, 0.10, 0.15, 0.30, 0.45 or 0.60) mL of $HAuCl_4$ (0.3 wt%) was added to 1 mL of 1 mg/mL UCNPs@PDA-$NaIO_4$ alkaline aqueous solution (pH 8.0) with ultrasonic treatment for 5 min. Finally, the obtained UCNPs@PDA-$NaIO_4$/Au were stored at 4 ℃.

## 2.5 Characterization

The Transmission Electron Microscope (TEM) and High-resolution Transmission Electron Microscope (HRTEM) images were provided by Titan G260-300 (FEI Company, USA). X-ray Diffraction (XRD) pattern was acquired by XD-6 diffractometer (Persee, China). The Upconversion Luminescence (UCL) spectra were characterized by a Dual-FL fluorescent spectrometer (HORIBA, Japan) using a 980 nm diode laser. Fourier Transform Infrared (FTIR) spectra were investigated on an Agilent Cary 660 FTIR spectrometer (Agilent, USA). X-ray Photoelectron Spectroscopy (XPS)

analyses were performed using K-Alpha (Thermo Fisher Scientific, USA). The Ultraviolet-visible (UV-vis) spectra were obtained from a Thermo UV-500 spectrophotometer (Thermo Fisher Scientific, USA). The Dynamic Light Scattering (DLS) was performed on a Zetasizer Nano-ZS90 (Malvern, UK). Thermogravimetric Analysis (TGA) curves were obtained from a TGA 5500 instrument (TA Instruments, USA).

# 3 Results and discussion

## 3.1. Preparation of UCNPs@PDA-oxidant ($NaIO_4$ or $O_2$)

The hydrophobic UCNPs were coated with PDA using the water-in-oil microemulsion method using ambient air or $NaIO_4$ as the oxidant. The corresponding representative TEM and HRTEM images are presented in Fig. 1. Fig. 1A, B shows that the UCNPs were uniform nanoparticles with an average diameter of 38.6 ± 0.2 nm. The fringe distance of 0.517 nm nicely matches well with the (1 1 1) plane of the hexagonal phase, $NaYF_4$ (JCPDS No. 28-1192), which is consistent with the XRD results (Fig. S1A). An approximately 2.9 nm PDA layer was uniformly deposited on UCNPs@PDA-$O_2$ prepared with ambient air as the oxidant (Fig. 1C, D); however, it takes too long (24 h) to complete the PDA coating because of the low chance of the ambient air to meeting the DA in the water-in-oil system. Thus, $NaIO_4$ was used instead of ambient air as the oxidant to improve the coating rate. The $NaIO_4$ solution comes in contact with the water to facilitate the oxidation of DA directly. Furthermore, the oxidizing ability of $NaIO_4$ is stronger than that of oxygen. Fig. 1E, F shows that an approximately 3 nm uniform PDA layer is consistently and uniformly deposited on the UCNPs@PDA-$NaIO_4$ synthesized using $NaIO_4$ as the oxidant with a reaction time of 10 min, and

without significant core-free PDA particles. The PDA layer of UCNPs@PDA-$NaIO_4$ synthesized by $NaIO_4$ oxidation for 2 h and 6 h was similar to the reaction time of 10 min (Fig. S2). In order to improve the experimental efficiency, the ideal reaction time was determined to be 10 min and was used subsequently. Furthermore, after coating with the PDA layer, the XRD patterns of UCNPs@PDA-$NaIO_4$ are similar to those of UCNPs (Fig. S1A), indicating that the PDA coating did not change the crystalline phase of $NaYF_4$. Fig. S1B shows that UCNPs@PDA-$NaIO_4$ lost 2.43% more weight than UCNPs, and which is the PDA coating. The UCL spectra of the UCNPs are shown in Fig. S1C, there are two green peaks (521 and 540 nm) and one red peak (657 nm) are attributed to energy transitions from $^2H_{11/2}$, $^4S_{3/2}$, and $^4F_{9/2}$ to $^4I_{15/2}$ of $Er^{3+}$ ions, respectively. After the UCNPs were coated with PDA, their UCL intensity decreased (Fig. S1C) because of the scattering effect on both emission and incident light by the PDA layer [39].

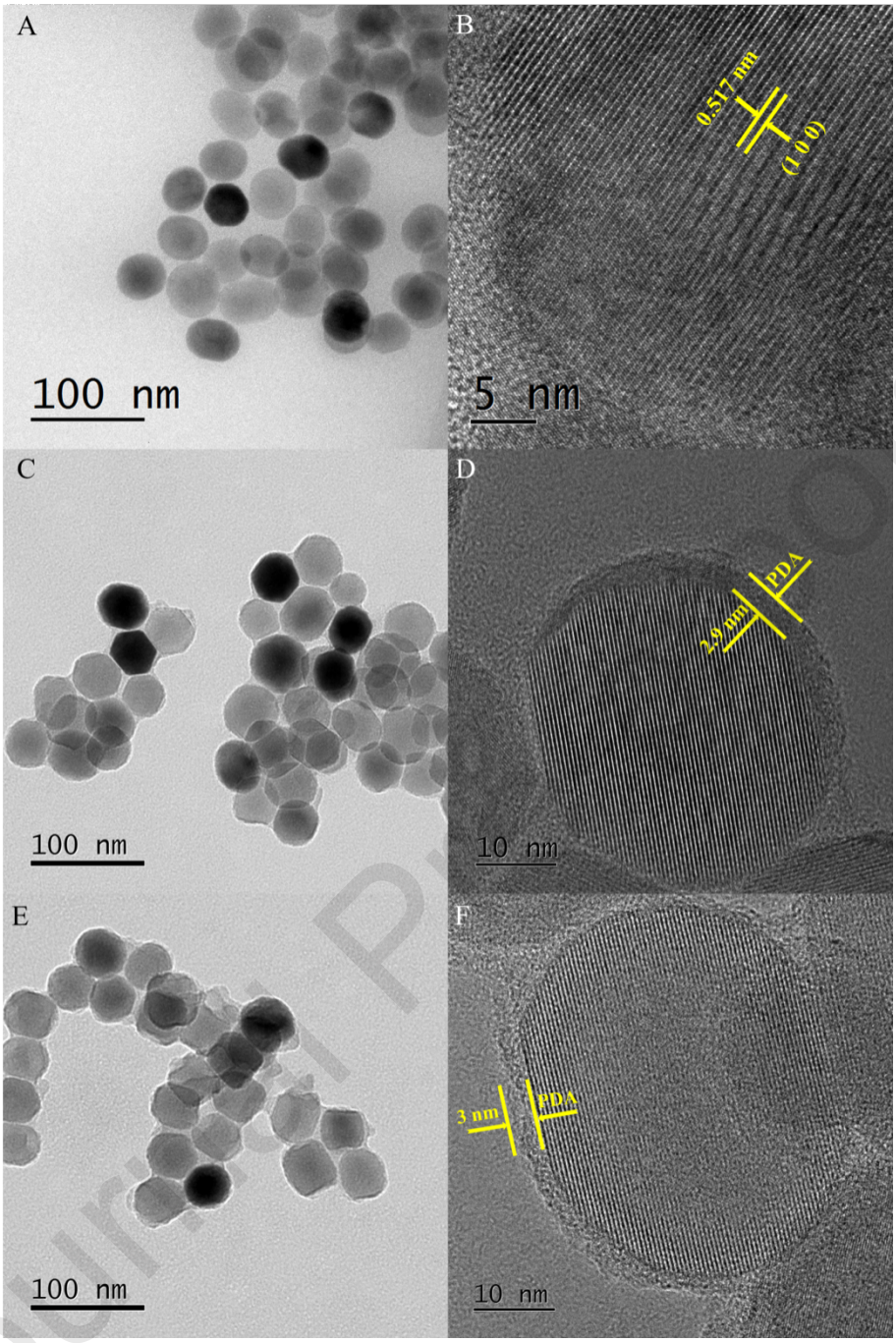


**Fig. 1.** TEM and HRTEM images of (A, B) UCNPs, (C, D) UCNPs@PDA-$O_2$ and (E, F) UCNPs@PDA-$NaIO_4$.

Interestingly, it was found that the dispersibility of the UCNPs@PDA-$NaIO_4$ obtained from the oxidation of DA for 10 min was much higher than that of UCNPs@PDA-$O_2$. The Zeta potentials of UCNPs@PDA-$O_2$ and UCNPs@PDA-$NaIO_4$ are shown in Fig. 2. The Zeta potentials of UCNPs@PDA-$O_2$ at pH 7.0 was –15.4 mV, which is in accordance with that reported in previous

studies [17]. However, the Zeta potentials of UCNPs@PDA-$NaIO_4$ at pH 7.0 was +26.4 mV. The difference in the Zeta potentials most probably originates from the difference in the compositions (and structures) of both kinds of PDA coatings. A comparative study of the coatings was carried out using FTIR and XPS to elucidate the difference between the compositions of PDA-$O_2$ and PDA-$NaIO_4$.

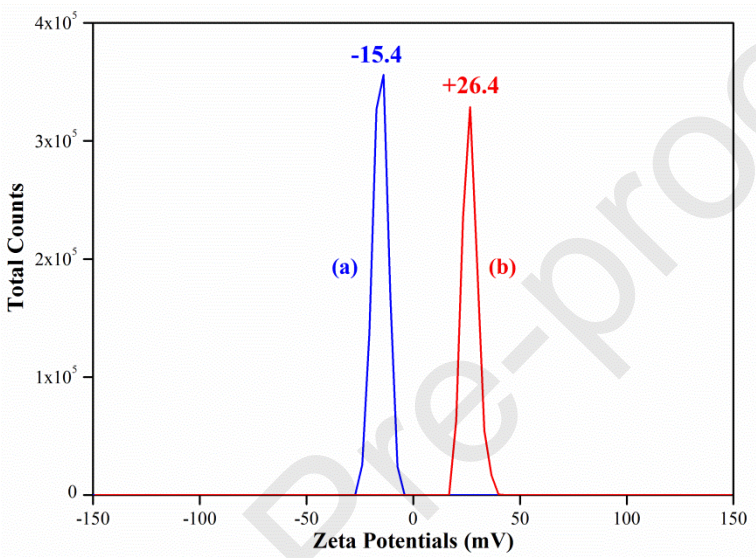


**Fig. 2.** Zeta potentials of (a) UCNPs@PDA-$O_2$ and (b) UCNPs@PDA-$NaIO_4$.

Fig. 3 shows the FTIR spectra. Bands at 1562 and 1445 $cm^{-1}$ are observed in the FTIR spectra of UCNPs, and may be attributed to the stretching vibration of the $COO^-$ groups [17]. After coating with PDA, the band corresponding to the $COO^-$ groups disappeared, indicating that ligand exchange would have taken place during PDA coating, according to the proposed mechanism using in silica coating in the water-in-oil microemulsion method [40, 41]. The spectra of PDA-coated UCNPs show new peaks at 1608, 1511 $cm^{-1}$ for UCNPs@PDA-$O_2$ and 1620, 1508 $cm^{-1}$ for UCNPs@PDA-$NaIO_4$. These may be attributed to the stretching vibration of the aromatic ring and the N–H shearing vibration of the amide group, respectively, indicating the formation of PDA coating on the UCNPs

[42]. The characteristic absorption peak of the C–O and C–O–H bonds (1123, 1246 $cm^{-1}$ for UCNPs@PDA-$O_2$ and 1072, 1253 $cm^{-1}$ for UCNPs@PDA-$NaIO_4$) appeared in the FTIR spectra of the two samples, indicating the existence of phenolic groups in the PDA coating [33, 43]. The intensity of the stretching vibration of the aromatic ring is a reference to show that the phenolic content in UCNPs@PDA-$NaIO_4$ is lower than that in UCNPs@PDA-$O_2$. When compared with that of UCNPs@PDA-$O_2$, the FTIR spectra of UCNPs@PDA-$NaIO_4$ shows a less pronounced peak, which may be attributed to the fact that PDA on UCNPs@PDA-$NaIO_4$ has a higher degree of oligomerization and self-assembly than that on UCNPs@PDA-$O_2$ [44]. In both products, the peaks between 800 and 880 $cm^{-1}$ attributed to the C–H wagging vibration of the ring hydrogens in the 1,2,4-trisubstituted and 1,2,4,5-tetrasubstitued benzenes [45] were observed; however, the position and intensity of the peak are different, indicating that there is a difference in the composition of the PDA-coated UCNPs prepared using different oxidants.

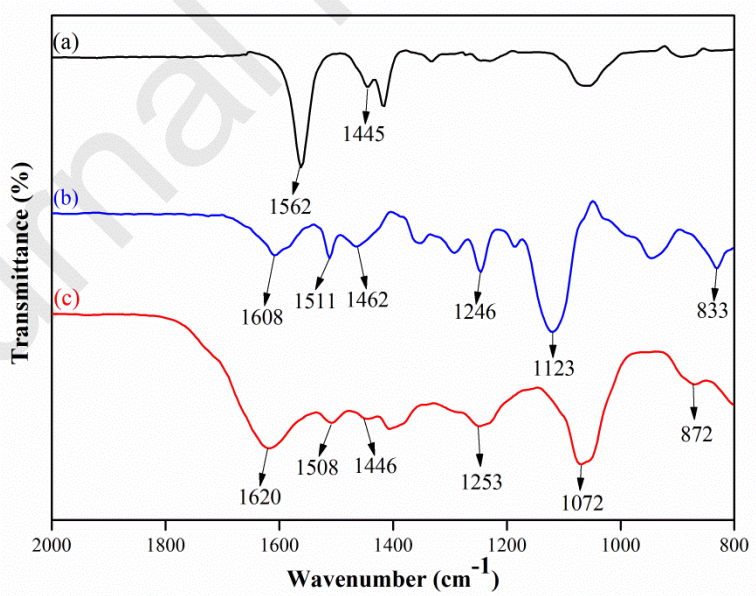


**Fig. 3.** FTIR spectra of (a) UCNPs, (b) UCNPs@PDA-$O_2$ and (c) UCNPs@PDA-$NaIO_4$.

Furthermore, XPS was used to characterize the elemental composition on the PDA coatings.

Fig. 4 shows the C 1s, N 1s core-level spectra of UCNPs@PDA-$O_2$ and UCNPs@PDA-$NaIO_4$. For both PDA coatings, the XPS C 1s core-level spectra can be curved-fitted into three peak components with binding energies of 284.36/284.33, 285.73/285.97, and 287.36/288.06 eV, corresponding to the C=C/C–C, C–O/C–N, and C=O species, respectively [46, 47]. The C=O content of the PDA-$NaIO_4$ coating is higher than that of PDA-$O_2$ coating, indicating the richer quinone groups in the PDA-$NaIO_4$ coating. By the deconvolution of the N 1s spectra of PDA-$O_2$ coating, two peaks at 397.16 and 401.03 eV, except that at 393.25 eV, were identified, which may be assigned to the R2-NH and R-$NH_2$ components, respectively [46, 47]. Compared with the PDA-$O_2$ coating, the ratio of R-$NH_2$/R2-NH of the PDA-$NaIO_4$ coating changed greatly, indicating the different composition of these two coatings. Additionally, the peak shifts of +1.47 eV are probably attributable to the protonation of R-$NH_2$ and pyrrolic R2-NH, owing to the fact that positive charging leads to an increase in the binding energy [47].

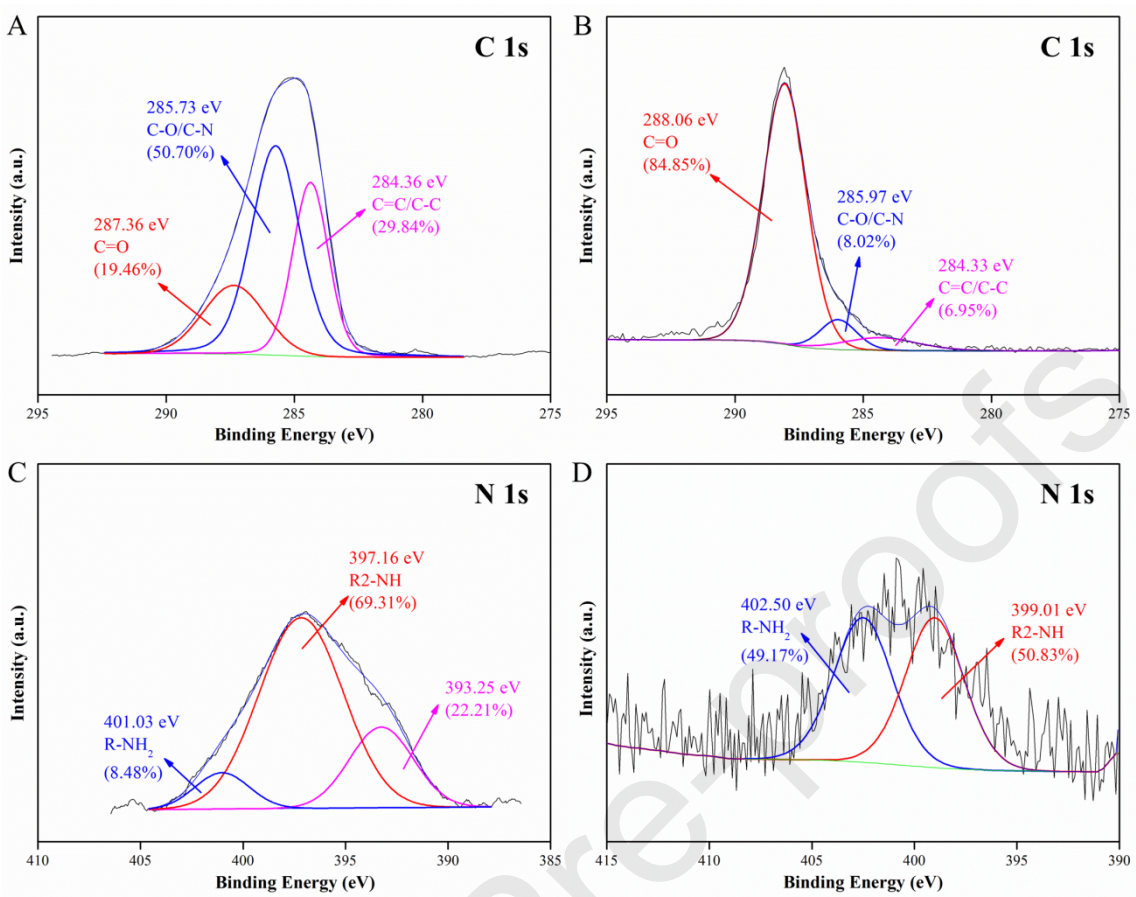


**Fig. 4.** XPS spectra of C 1s, N 1s core levels of (A, C) UCNPs@PDA-$O_2$ and (B, D) UCNPs@PDA-$NaIO_4$.

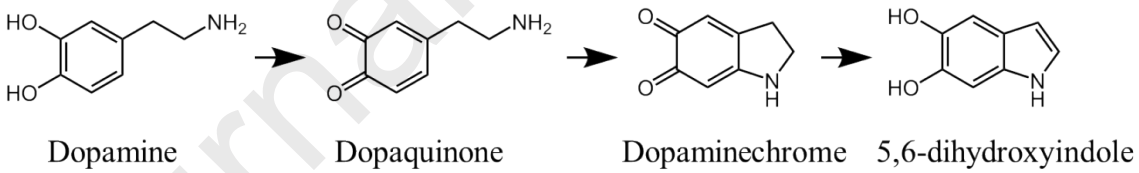


**Scheme 2.** The initial stages of PDA coating formation

There is general agreement that the initial stages (as shown in Scheme 2) of PDA coating formation involves auto-oxidation of DA giving rise to dopaquinone (DQ), followed by an intramolecular Michael addition and deprotonation leading to leuco-dopaminechrome [13, 48-51]. Additional oxidation and rearrangement leads to the formation of indole quinone, which then rearranges to form 5,6-dihydroxyindole (DHI)—a key precursor to PDA [13, 48-51]. Although the

initial pH of reactions systems were adjusted to 8.0 equally, the pH of suspensions with $NaIO_4$ as the oxidant moved to a more acidic value than that of $O_2$ as the oxidant. This is the result of more hydrogen atom abstraction from DA as the oxidation of DA progressed when $NaIO_4$ was used as the oxidant, leading to protonation of the amines of DA or DQ [47, 52]. Protonating the amines of DA or DQ prevents the intramolecular Michael addition, which make the ratio of R-$NH_2$/R2-NH of the PDA-$NaIO_4$ coating higher than that of PDA-$O_2$ coating. The exact process of $NaIO_4$-induced DA oxidation polymerization to form PDA will be studied in our future work.

Despite the fact that the chemical composition of the PDA has not been fully elucidated, certain functional groups are known to be present in the polymer, including catechol, quinone, and amines [53]. The surface charge on the PDA coating may originate from the dissociation of the amine and catechol [54]. These results suggest that the relatively low phenol content of the PDA-$NaIO_4$ coating and the variation in the protonation ability of amines caused by the different compositions of the two coatings might make UCNPs@PDA-$NaIO_4$ positively charged relative to UCNPs@PDA-$O_2$. Another important factor that affects the charge of the PDA coating perhaps is the higher rate of hydrogen atom abstraction from DA as the oxidation of DA progressed when $NaIO_4$ was used as the oxidant, thus protonating the amines in the PDA-$NaIO_4$ coating [47]. Interestingly, PDA microspheres (PDA MPs), PDA-coated OA-stabilized $Fe_3O_4$ (OA-$Fe_3O_4$@PDA-$NaIO_4$), and PDA-coated OAm-stabilized Au (OAm-Au@PDA-$NaIO_4$) were synthesized using the water-in-oil microemulsion method using $NaIO_4$ as the oxidant; the Zeta potentials of the three products were all positive (Fig. S3). The results indicate that $NaIO_4$ as an oxidant not only rapidly forms a PDA coating but also obtains nanoparticles with a positively charged surface, an observation that has not been made in previous studies.

Stability is crucial in practical applications. Thus, we characterized its UCL stability, and the results are shown in Fig. 5. It can be seen that after 30 days, the UCL wavelengths (521, 540, and 657 nm) of UCNPs@PDA-$NaIO_4$ changed barely, indicating that UCNPs@PDA-$NaIO_4$ has good stability. This is because PDA consists of hydrophilic hydroxyl and amino groups, which improves the stability of UCNPs@PDA-$NaIO_4$ [30, 55, 56].

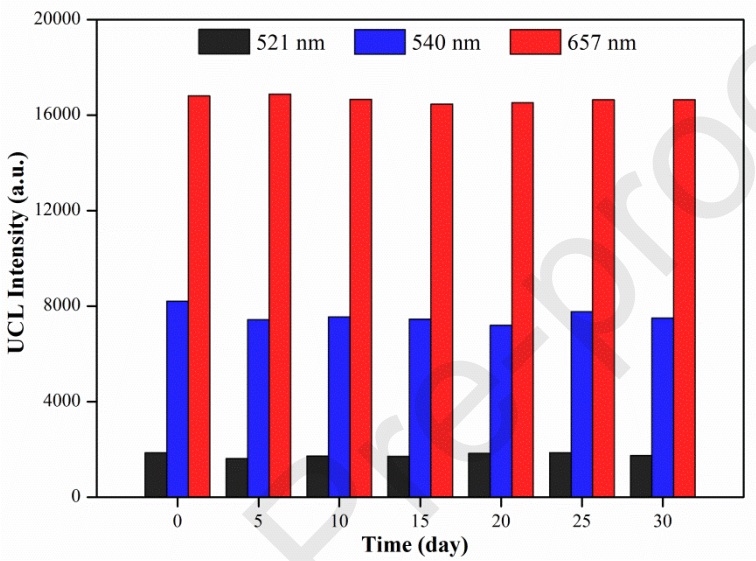


**Fig. 5.** The stability of UCNPs@PDA-$NaIO_4$ at UCL wavelengths of 521 nm, 540 nm, and 657 nm.

## 3.2. Preparation of UCNPs@PDA-$NaIO_4$/Au

PDA coatings can act as reactive templates, and can facilitate the one-pot synthesis of UCNP-supported Au NPs. Although most of the results on the immobilization of Au NPs on PDA coatings have been reported, little attention has been paid to the effect of pH on the loading process. The TEM results of the products obtained at pH 4.0 and 8.0 during the loading of Au NPs on the surface of UCNPs@PDA-$NaIO_4$ are below. A small number of free Au NPs are observed at pH 4.0 (Fig. 6A). It is clear that all of the Au NPs are located on the surface of UCNPs@PDA-$NaIO_4$

without forming large aggregates, and that no individual Au NPs were found in the solution at pH 8.0 (Fig. 6B). A similar phenomenon was observed when UCNPs@PDA-$NaIO_4$ were replaced with OA-$Fe_3O_4$@PDA-$NaIO_4$ (Fig. S4). The mechanism for loading Au NPs on OA-$Fe_3O_4$@PDA was proposed in our previous work [42]. The strong chelating ability of *ortho*-phenolic hydroxyls with Au (III) prompted the dissociation of some PDA molecules from the $Fe_3O_4$ core surface, and the dissociated PDA molecules reduced Au (III) to form Au NPs, which were then loaded on to the surface of PDA-coated $Fe_3O_4$ NPs [42]. At pH 4.0, the Zeta potentials of the side solution after magnetic separation were +12.7 mV (Fig. S3D) indicating that the formed Au NPs could not attach themselves on to the surface of UCNPs@PDA-$NaIO_4$ due to the electrostatic repulsion between them and UCNPs@PDA-$NaIO_4$ [57].

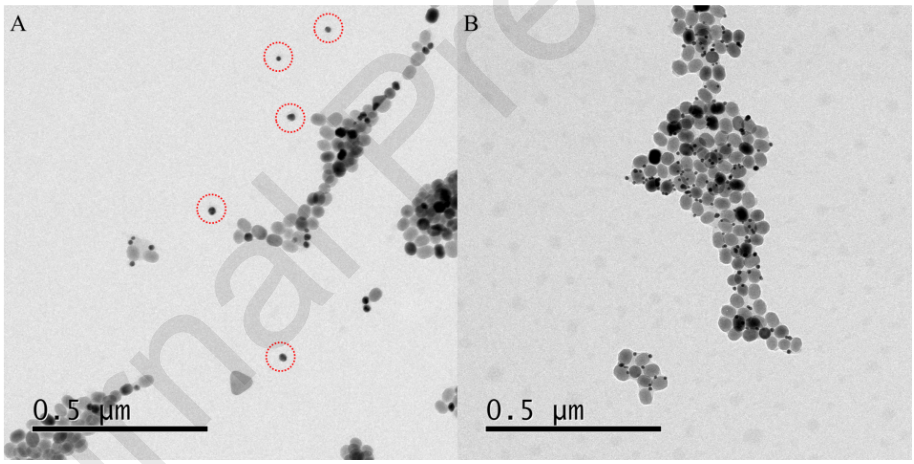


**Fig. 6.** TEM images of UCNPs@PDA-$NaIO_4$/Au synthesized at (A) pH 4.0 and (B) pH 8.0.

To investigate the amount of immobilized Au NPs on UCNPs@PDA-$NaIO_4$, we carried out a series of experiments by changing the dosage of $HAuCl_4$. Representative TEM images are presented in Fig. 7. It shows that the average diameter of Au NPs was 8.1 ± 1.2 nm, and the density of Au NPs increased when the dosage of $HAuCl_4$ increased. The UV–vis spectra in Fig. 8A shows that the UCNPs@PDA-$NaIO_4$ had no apparent absorption, and a red shift in the absorption peak of

UCNPs@PDA-$NaIO_4$/Au was observed with the increase in the dosage of Au. That is, the surface plasmon resonance (SPR) frequency of Au NPs was shifted to higher wavelengths, which may be attributed to the increased loading density of Au NPs and the formation of small Au clusters [58, 59].

Plasmonic metal nanostructures (usually Ag and Au) placed in close proximity to UCNPs have been demonstrated to be excellent tools for tuning UCL by enhancing or quenching the luminescence intensity [58-64]. Fig. 8B shows that the Au NPs load does not change the peak pattern of UCL spectra, only the UCL intensity changes; the enhancement factor for different UCL wavelengths are shown in Fig. 8C. Notably, the enhancement factor of the red peak (657 nm) reached 10.19 when the dosage of $HAuCl_4$ was 0.15 mL. The SPR frequency of Au NPs matches the UCL wavelength of UCNPs (540 nm) resulting in SPR coupling and local electric field enhancement, which effectively improves emission efficiency and enhances UCL intensity [58-64]. However, the fluorescence enhancement decreased when the dosage of $HAuCl_4$ increased, which may be due to the transfer of non-radiative energy from UCNPs to Au NPs [58-64] or the enhancement of the internal filtration effect [58]. Fig. 7 and Fig. 8 reveal that Au nanoparticles with different load densities can be achieved by changing the dosage of $HAuCl_4$, thereby achieving the goal of regulating the UCL intensity of UCNPs.

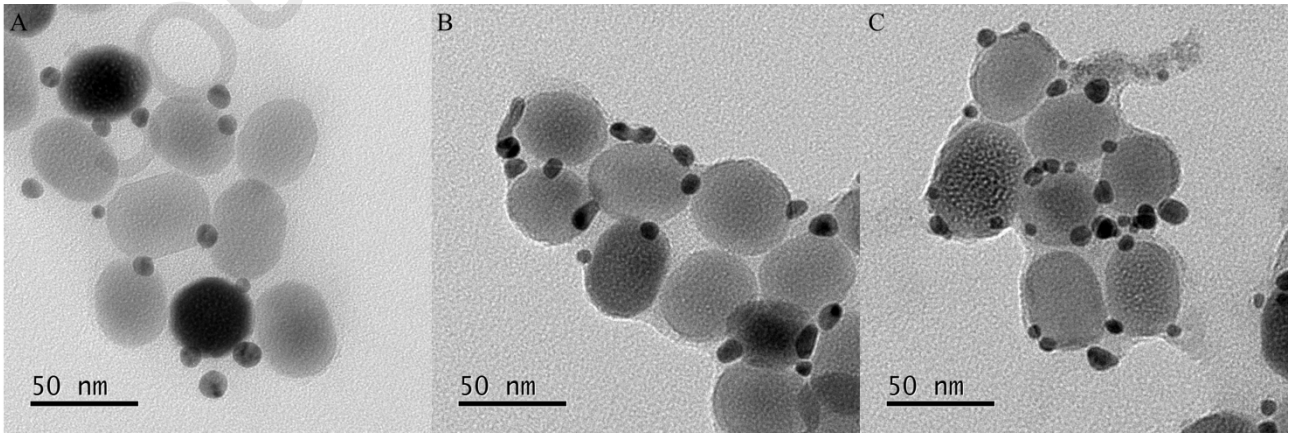


**Fig. 7.** TEM images of UCNPs@PDA-$NaIO_4$/Au synthesized at pH 8.0 with (A) 0.15 mL, (B) 0.30 mL and (C) 0.60 mL of $HAuCl_4$.

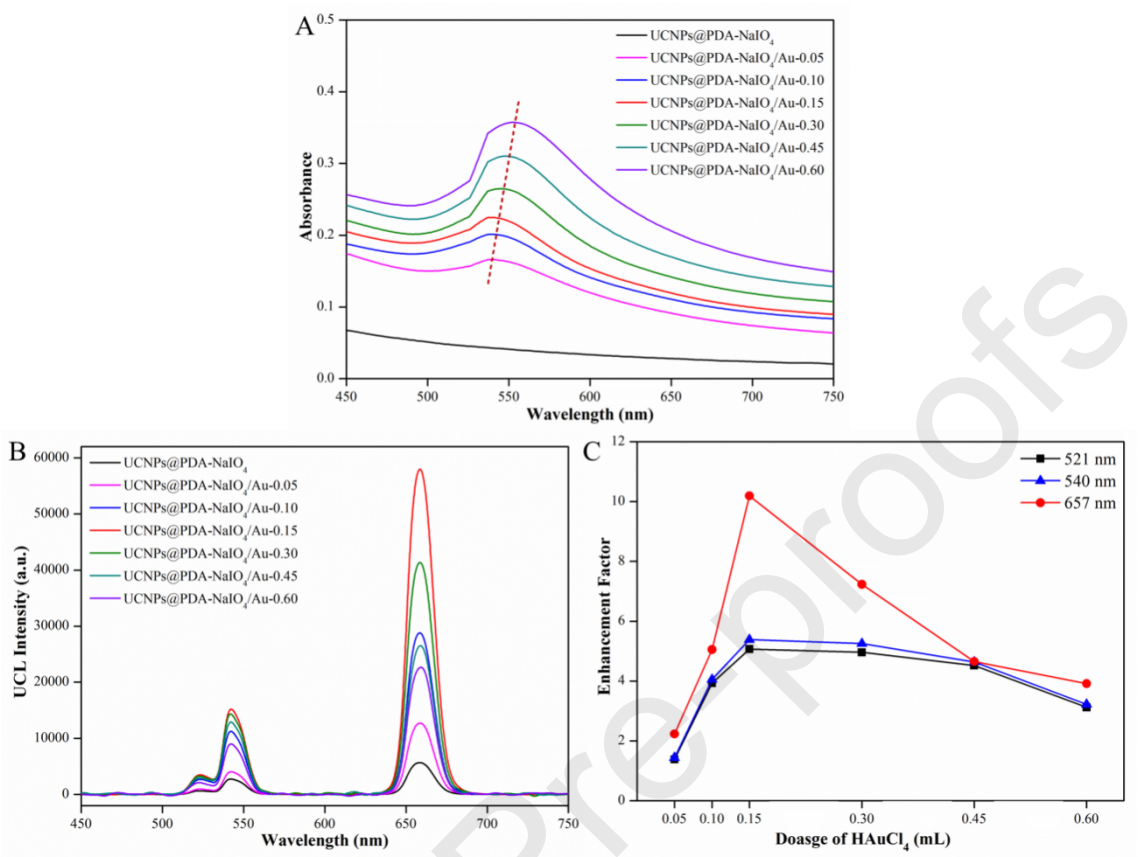


**Fig. 8.** (A) UV-vis spectra, (B) UCL spectra and (C) UCL enhancement of UCNPs@PDA-$NaIO_4$/Au synthesized at pH 8.0 with different dosage of $HAuCl_4$.

# 4 Conclusions

In summary, hydrophobic UCNPs with a uniform morphology were synthesized via a thermal decomposition method. Rapid oxidative polymerization of DA on UCNPs was induced by $NaIO_4$ in a water-in-oil microemulsion system, resulting in positively charged water-soluble UCNPs@PDA-$NaIO_4$ nanocomposites that can be stably stored for 30 days. Subsequently, $HAuCl_4$ was reduced *in situ* to Au NPs by PDA coating on the surface of UCNPs at pH 8.0, and UCNPs@PDA-$NaIO_4$/Au nanocomposites were obtained, which could effectively enhance the UCL

intensity. In addition, the surface Au NPs load density of UCNPs@PDA-$NaIO_4$ can be adjusted by changing the dosage of $HAuCl_4$. It is expected that the nanocomposites with unique properties will enable their wide implementation in biological imaging, diagnostic analysis and other biological fields.

**Corresponding Author**

* liudeming@ciomp.ac.cn; polymerzf@swun.cn

**Author Contributions**

**Wei Zhang:** Conceptualization, Methodology, Investigation, Validation, Writing-Original Draft, Writing-Review & Editing. **Zhengfang Liao:** Methodology, Investigation, Validation. **Xiaoqi Meng:** Investigation, Formal Analysis. **A Erpuding · Ai Niwaer:** Validation. **Hongyue Wang:** Formal Analysis. **Xinhua Li:** Project Administration. **Deming Liu:** Conceptualization, Supervision, Project Administration, Writing-Review & Editing. **Fang Zuo:** Conceptualization, Supervision, Project Administration, Writing-Review & Editing, Resources.

**Notes**

The authors declare no competing financial interest.

**Acknowledgments**

This work was supported by the National Natural Science Foundation of China (51273220, 11727902), the Sichuan Provincial Department of Education Project (18ZA0510), and the Fundamental Research Funds for the Central Universities (2020NZD01), Southwest Minzu University. We thank LetPub (www.letpub.com) for linguistic assistance during the preparation of this manuscript.

**References**

[1] Y. M. Yang, Q. Shao, R. R. Deng, C. Wang, X. Teng, K. Cheng, Z. Cheng, L. Huang, Z. Liu, X. G. Liu, B. G. Xing, In vitro and in vivo uncaging and bioluminescence imaging by using photocaged upconversion nanoparticles, Angew. Chem. Int. Edit. 51 (2012) 3125-3129.

[2] H. Rabie, Y. X. Zhang, N. Pasquale, M. J. Lagos, P. E. Batson, K. B. Lee, NIR biosensing of neurotransmitters in stem cell-derived neural interface using advanced core-shell upconversion nanoparticles, Adv. Mater. 31 (2019) 1806991.

[3] H. Y. Peng, B. B. Ding, Y. C. Ma, S. Q. Sun, W. Tao, Y. C. Guo, H. C. Guo, X. Z. Yang, H. S. Qian, Sequential growth of sandwiched $NaYF_4$:Yb/Er@$NaYF_4$:Yb@$NaNdF_4$:Yb core-shell-shell nanoparticles for photodynamic therapy, Appl. Surf. Sci. 357 (2015) 2408-2414.

[4] Z. Y. Chen, G. X. Liu, J. T. Sui, D. Li, Y. Song, F. Hong, X. T. Dong, J. X. Wang, W. S. Yu, Multifunctional PVP-$Ba_2GdF_7$:$Yb^{3+}$,$Ho^{3+}$ coated on Ag nanospheres for bioimaging and tumor photothermal therapy, Appl. Surf. Sci. 458 (2018) 931-939.

[5] F. Wang, S. H. Wen, H. He, B. M. Wang, Z. G. Zhou, O. Shimoni, D. Y. Jin, Microscopic inspection and tracking of single upconversion nanoparticles in living cells, Light-Sci. Appl. 7 (2018) 18007.

[6] V. Muhr, S. Wilhelm, T. Hirsch, O. S. Wolfbeis, Upconversion nanoparticles: From hydrophobic to hydrophilic surfaces, Accounts Chem. Res. 47 (2014) 3481-3493.

[7] Z. G. Chen, H. L. Chen, H. Hu, M. X. Yu, F. Y. Li, Q. Zhang, Z. G. Zhou, T. Yi, C. H. Huang, Versatile synthesis strategy for carboxylic acid-functionalized upconverting nanophosphors as biological labels, J. Am. Chem. Soc. 130 (2008) 3023-3029.

[8] H. P. Zhou, C. H. Xu, W. Sun, C. H. Yan, Clean and flexible modification strategy for carboxyl/aldehyde-functionalized upconversion nanoparticles and their optical applications, Adv. Funct. Mater. 19 (2009) 3892-3900.

[9] W. Kong, T. Y. Sun, B. Chen, X. Chen, F. J. Ai, X. Y. Zhu, M. Y. Li, W. J. Zhang, G. Y. Zhu, F. Wang, A general strategy for ligand exchange on upconversion nanoparticles, Inorg. Chem. 56 (2017) 872-877.

[10] Z. L. Qin, S. N. Du, Y. Luo, Z. J. Liao, F. Zuo, J. B. Luo, D. Liu, Hydrothermal synthesis of superparamagnetic and red luminescent bifunctional $Fe_3O_4$@$Mn^{2+}$-doped $NaYF_4$:Yb/Er core@shell monodisperse nanoparticles and their subsequent ligand exchange in water, Appl. Surf. Sci. 378 (2016) 174-180.

[11] Y. Luo, S. N. Du, W. Zhang, Z. F. Liao, F. Zuo, S. T. Yang, Core@shell $Fe_3O_4$@$Mn^{2+}$-doped $NaYF_4$:Yb/Tm nanoparticles for triple-modality $T_1/T_2$-weighted MRI and NIR-to-NIR upconversion luminescence imaging agents, RSC Adv. 7 (2017) 37929-37937.

[12] R. Abdul Jalil, Y. Zhang, Biocompatibility of silica coated $NaYF_4$ upconversion fluorescent nanocrystals, Biomaterials 29 (2008) 4122-4128.

[13] H. Lee, S. M. Dellator, W. M. Miller, P. B. Messersmith, Mussel-inspired surface chemistry for multifunctional coatings, Science 318 (2007) 426-430.

[14] T. G. Barclay, H. M. Hegab, S. R. Clarke, M. Ginic Markovic, Versatile surface modification using polydopamine and related polycatecholamines: Chemistry, structure, and applications, Adv. Mater. Interfaces 4 (2017) 1601192.

[15] W. Cheng, J. P. Nie, N. S. Gao, G. Liu, W. Tao, X. J. Xiao, L. J. Jiang, Z. G. Liu, X. W. Zeng, L. Mei, A multifunctional nanoplatform against multidrug resistant cancer: Merging the best of

targeted chemo/gene/photothermal therapy, Adv. Funct. Mater. 27 (2017) 1704135.

[16] Y. M. Peng, J. P. Nie, W. Cheng, G. Liu, D. W. Zhu, L. H. Zhang, C. Y. Liang, L. Mei, L. Q. Huang, X. W. Zeng, A multifunctional nanoplatform for cancer chemo-photothermal synergistic therapy and overcoming multidrug resistance, Biomater. Sci. 6 (2018) 1084-1098.

[17] F. Y. Liu, X. X. He, Z. Lei, L. Liu, J. P. Zhang, H. P. You, H. M. Zhang, Z. X. Wang, Facile preparation of doxorubicin-loaded upconversion@polydopamine nanoplatforms for simultaneous in vivo multimodality imaging and chemophotothermal synergistic therapy, Adv. Healthc. Mater. 4 (2015) 559-568.

[18] L. Ma, F. Y. Liu, Z. Lei, Z. X. Wang, A novel upconversion@polydopamine core@shell nanoparticle based aptameric biosensor for biosensing and imaging of cytochrome c inside living cells, Biosens. Bioelectron. 87 (2017) 638-645.

[19] Y. Dai, D. P. Yang, D. Yu, C. Cao, Q. H. Wang, S. H. Xie, L. Shen, W. Feng, F. Y. Li, Mussel-inspired polydopamine-coated lanthanide nanoparticles for NIR-II/CT dual imaging and photothermal therapy, ACS Appl. Mater. Interfaces 9 (2017) 26674-26683.

[20] X. L. Li, M. Y. Jiang, S. J. Zeng, H. R. Liu, Polydopamine coated multifunctional lanthanide theranostic agent for vascular malformation and tumor vessel imaging beyond 1500 nm and imaging-guided photothermal therapy, Theranostics 9 (2019) 3866-3878.

[21] J. Yan, L. P. Yang, M. F. Lin, J. Ma, X. H. Lu, P. S. Lee, Polydopamine spheres as active templates for convenient synthesis of various nanostructures, Small 9 (2013) 596-603.

[22] S. X. Lu, J. Y. Yu, Y. Y. Cheng, Q. Wang, A. Barras, W. G. Xu, S. Szunerits, D. Cornu, R. Boukherroub, Preparation of silver nanoparticles/polydopamine functionalized polyacrylonitrile fiber paper and its catalytic activity for the reduction 4-nitrophenol, Appl. Surf. Sci. 411 (2017)

163-169.

[23] S. N. Du, Y. Luo, F. Zuo, X. H. Li, D. Liu, Polydopamine-coated $Fe_3O_4$ nanoparticles as synergistic redox mediators for catalytic reduction of azo dyes, Nano 12 (2017) 1750037.

[24] S. N. Du, Y. Luo, Z. F. Liao, W. Zhang, X. H. Li, T. Y. Liang, F. Zuo, K. Y. Ding, New insights into the formation mechanism of gold nanoparticles using dopamine as a reducing agent, J. Colloid Interface Sci. 523 (2018) 27-34.

[25] J. Y. Duan, L. F. Bai, K. Z. Xu, Q. L. Fang, Y. H. Sun, H. Xu, K. C. Leung, S. H. Xuan, Polydopamine protected hollow nanosphere with AuAg-nanoframe-core@carbon@AuAg-nanocrystals-satellite hybrid nanostructure (AuAg@C@AuAg/PDA) for enhancing nanocatalysis, J. Hazard. Mater. 384 (2020) 121276.

[26] M. Zhang, X. W. He, L. X. Chen, Y. K. Zhang, Preparation of IDA-Cu functionalized core-satellite $Fe_3O_4$/polydopamine/Au magnetic nanocomposites and their application for depletion of abundant protein in bovine blood, J. Mate. Chem. 20 (2010) 10696-10704.

[27] B. Wang, M. Zhang, W. Z. Li, L. L. Wang, J. Zheng, W. J. Gan, J. L. Xu, Fabrication of Au(Ag)/AgCl/$Fe_3O_4$@PDA@Au nanocomposites with enhanced visible-light-driven photocatalytic activity, Dalton. Trans. 44 (2015) 17020-17025.

[28] C. Qi, L. H. Fu, H. Xu, T. F. Wang, J. Lin, P. Huang, Melanin/polydopamine-based nanomaterials for biomedical applications, Sci. China-Chem. 62 (2019) 162-188.

[29] W. Cheng, X. W. Zeng, H. Z. Chen, Z. M. Li, W. F. Zeng, L. Mei, Y. L. Zhao, Versatile polydopamine platforms: Synthesis and promising applications for surface modification and advanced nanomedicine, ACS Nano 13 (2019) 8537-8565.

[30] C. Zhang, Y. Ou, W. X. Lei, L. S. Wan, J. Ji, Z. K. Xu, $CuSO_4$/$H_2O_2$-induced rapid deposition

of polydopamine coatings with high uniformity and enhanced stability, Angew. Chem. Int. Edit. 55 (2016) 3054 -3057.

[31] M. Salomäk, L. Marttila, Kivelä, H., T. Ouvinen, J. Lukkari, Effects of pH and oxidants on the first steps of polydopamine formation: A thermodynamic approach, J. Phys. Chem. B 122 (2018) 6314-6327.

[32] F. Ponzio, J. Barthès, J. Bour, M. Michel, P. Bertani, J. Hemmerlé, M. d'Ischia, V. Ball, Oxidant control of polydopamine surface chemistry in acids: A mechanism-based entry to superhydrophilic-superoleophobic coatings, Chem. Mat. 28 (2016) 4697-4705.

[33] C. D. Luo, Q. X. Liu, Oxidant-induced high-efficient mussel-inspired modification on PVDF membrane with superhydrophilicity and underwater superoleophobicity characteristics for oil/water separation, ACS Appl. Mater. Interfaces 9 (2017) 8297-8307.

[34] J. Q. Wang, H. Guo, X. N. Shi, Z. K. Yao, W. H. Qing, F. Liu, C. Y. Tang, Fast polydopamine coating on reverse osmosis membrane: Process investigation and membrane performance study, J. Colloid Interface Sci. 535 (2019) 239-244.

[35] G. G. Sun, F. S. Zu, N. Koch, J. Rappich, K. Hinrichs, In situ infrared spectroscopic monitoring and characterization of the growth of polydopamine (PDA) films, Phys. Status Solidi B 256 (2019) 1800308.

[36] L. P. Yang, J. H. Kong, D. Zhou, J. M. Ang, S. L. Phua, W. A. Yee, H. Liu, Y. Z. Huang, X. H. Lu, Transition-metal-ion-mediated polymerization of dopamine: Mussel-inspired approach for the facile synthesis of robust transition-metal nanoparticle-graphene hybrids, Chem.-Eur. J. 20 (2014) 7776-7683.

[37] L. Ding, M. Zhang, Y. W. Zhang, J. B. Yang, J. Zheng, J. L. Xu, A type of raspberry-like silica

composite with tunable nickel nanoparticles coverage towards nanocatalysis and protein adsorption, Green Chem. 18 (2016) 6282-6290.

[38] D. M. Liu, X. X. Xu, Y. Du, X. Qin, Y. H. Zhang, C. S. Ma, S. H. Wen, W. Ren, E. M. Goldys, J. A. Piper, S. X. Dou, X. G. Liu, D. Y. Jin, Three-dimensional controlled growth of monodisperse sub-50 nm heterogeneous nanocrystals, Nat. Commun. 7 (2016) 10254.

[39] X. J. Huang, B. Li, C. Peng, G. S. Song, Y. X. Peng, Z. Y. Xiao, X. J. Liu, J. M. Yang, L. Yu, J. Q. Hu, $NaYF_4$:Yb/Er@PPy core-shell nanoplates: An imaging-guided multimodal platform for photothermal therapy of cancers, Nanoscale 8 (2016) 1040-1048.

[40] H. L. Ding, Y. X. Zhang, S. Wang, J. M. Xu, S. C. Xu, G. H. Li, $Fe_3O_4$@$SiO_2$ core/shell nanoparticles: The silica coating regulations with a single core for different core sizes and shell thicknesses, Chem. Mat. 24 (2012) 4572-4580.

[41] R. Koole, M. M. van Schooneveld, J. Hilhorst, C. de Mello Donegá, D. C. ’t Hart, A. van Blaaderen, D. Vanmaekelbergh, A. Meijerink, On the incorporation mechanism of hydrophobic quantum dots in silica spheres by a reverse microemulsion method, Chem. Mat. 20 (2008) 2503-2512.

[42] P. An, F. Zuo, X. H. Li, Y. P. Wu, J. H. Zhang, Z. H. Zheng, X. B. Ding, Y. X. Peng, A bio-inspired polydopamine approach to preparation of gold-coated $Fe_3O_4$ core-shell nanoparticles: Synthesis, characterization and mechanism, Nano 8 (2013) 1350061.

[43] J. W. Fu, Q. Q. Xin, X. C. Wu, Z. H. Chen, Y. Yan, S. J. Liu, M. H. Wang, Q. Xu, Selective adsorption and separation of organic dyes from aqueous solution on polydopamine microspheres, J. Colloid Interface Sci. 461 (2016) 292-304.

[44] J. H. Lin, C. J. Yu, Y. C. Yang, W. L. Tseng, Formation of fluorescent polydopamine dots from

hydroxyl radical-induced degradation of polydopamine nanoparticles, Phys. Chem. Chem. Phys. 17 (2015) 15124-15130.

[45] A. Ghanbari, F. Warchomicka, C. Sommitsch, A. Zamanian, Investigation of the oxidation mechanism of dopamine functionalization in an AZ31 magnesium alloy for biomedical applications, Coatings 9 (2019) 584.

[46] M. B. Clark, J. A. Gardella, T. M. Schultz, D. G. Patil, L. Salvati, Solid-state analysis of eumelanin biopolymers by electron spectroscopy for chemical analysis, Anal. Chem. 62 (1990) 949-956.

[47] Y. Xuan, G. C. Jiang, Y. Y. Li, J. S. Wang, H. N. Geng, Inhibiting effect of dopamine adsorption and polymerization on hydrated swelling of montmorillonite, Colloid Surf. A-Physicochem. Eng. Asp. 422 (2013) 50-60.

[48] P. Delparastan, K. G. Malollari, H. Lee, P. B. Messersmith, Direct evidence for the polymeric nature of polydopamine, Angew. Chem. Int. Edit. 58 (2019) 1077-1082.

[49] N. F. Della Vecchia, R. Avolio, M. Alfè, M. E. Errico, A. Napolitano, M. d'Ischia, Building-block diversity in polydopamine underpins a multifunctional eumelanin-type platform tunable through a quinone control point, Adv. Funct. Mater. 23 (2013) 1331-1340.

[50] J. E. Lemaster, A. S. Jeevarathinam, A. Kumar, B. Chandrasekar, F. Chen, J. V. Jokerst, Synthesis of ultrasmall synthetic melanin nanoparticles by UV irradiation in acidic and neutral conditions, ACS Appl. Bio Mater. 2 (2019) 4667-4674.

[51] W. Tao, X. W. Zeng, J. Wu, X. Zhu, X. H. Yu, X. D. Zhang, J. X. Zhang, G. Liu, L. Mei, Polydopamine-based surface modification of novel nanoparticle-aptamer bioconjugates for in vivo breast cancer targeting and enhanced therapeutic effects, Theranostics 6 (2016) 470-484.

[52] K. Y. Ju, Y. Lee, S. Lee, S. B. Park, J. K. Lee, Bioinspired polymerization of dopamine to generate melanin-like nanoparticles having an excellent free-radical-scavenging property, Biomacromolecules 12 (2011) 625-632.

[53] G. Pérez Mitta, J. S. Tuninetti, W. Knoll, C. Trautmann, M. E. Toimil Molares, O. Azzaroni, Polydopamine meets solid-state nanopores: A bioinspired integrative surface chemistry approach to tailor the functional properties of nanofluidic diodes, J. Am. Chem. Soc. 137 (2015) 6011-6017.

[54] H. Karkhanechi, R. Takagi, H. Matsuyama, Biofouling resistance of reverse osmosis membrane modified with polydopamine, Desalination 336 (2014) 87-96.

[55] L. P. Zhu, J. H. Jiang, B. K. Zhu, Y. Y. Xu, Immobilization of bovine serum albumin onto porous polyethylene membranes using strongly attached polydopamine as a spacer, Colloid Surf. B-Biointerfaces 86 (2011) 111-118.

[56] V. K. Thakur, J. Yan, M. F. Lin, C. Y. Zhi, D. Golberg, Y. Bando, R. Sim, P. S. Lee, Novel polymer nanocomposites from bioinspired green aqueous functionalization of BNNTs, Polym. Chem. 3 (2012) 962-969.

[57] H. L. Xu, X. K. Liu, G. Su, B. Zhang, D. Y. Wang, Electrostatic repulsion-controlled formation of polydopamine-gold janus particles, Langmuir 28 (2012) 13060-13065.

[58] X. J. Niu, H. Y. Chen, Y. Q. Wang, W. H. Wang, X. Y. Sun, L. X. Chen, Upconversion fluorescence-SERS dual-mode tags for cellular and in vivo imaging, ACS Appl. Mater. Interfaces 6 (2014) 5152-5160.

[59] H. Zhang, Y. J. Li, I. A. Ivanov, Y. Q. Qu, Y. Huang, X. F. Duan, Plasmonic modulation of the upconversion fluorescence in $NaYF_4$:Yb/Tm hexaplate nanocrystals using gold nanoparticles or

nanoshells, Angew. Chem. Int. Edit. 49 (2010) 2865-2868.

[60] D. G. Yin, C. C. Wang, J. Ouyang, X. Y. Zhang, Z. Jiao, Y. Feng, K. L. Song, B. Liu, X. Z. Cao, L. Zhang, Y. L. Han, M. H. Wu, Synthesis of a novel core-shell nanocomposite Ag@$SiO_2$@$Lu_2O_3$:Gd/Yb/Er for large enhancing upconversion luminescence and bioimaging, ACS Appl. Mater. Interfaces 6 (2014) 18480-18488.

[61] W. Park, D. Lu, S. Ahn, Plasmon enhancement of luminescence upconversion, Chem. Soc. Rev. 44 (2015) 2940-2962.

[62] Z. Q. Li, L. M. Wang, Z. Y. Wang, X. H. Liu, Y. J. Xiong, Modification of $NaYF_4$:Yb,Er@$SiO_2$ nanoparticles with gold nanocrystals for tunable green-to-red upconversion emissions, J. Phys. Chem. C 115 (2011) 3291-3296.

[63] P. Y. Yuan, Y. H. Lee, M. K. Gnanasammandhan, Z. P. Guan, Y. Zhang, Q. H. Xu, Plasmon enhanced upconversion luminescence of $NaYF_4$:Yb,Er@$SiO_2$@Ag core-shell nanocomposites for cell imaging, Nanoscale 4 (2012) 5132-5137.

[64] D. Mendez Gonzalez, S. Melle, O. G. Calderón, M. Laurenti, E. Cabrera Granado, A. Egatz Gómez, E. López Cabarcos, J. Rubio Retama, E. Díaz, Control of upconversion luminescence by gold nanoparticle size: From quenching to enhancement, Nanoscale 11 (2019) 13832-13844.

The manuscript was written through contributions of all authors. All authors have given approval to the final version of the manuscript.

**Author Contributions**

**Wei Zhang:** Conceptualization, Methodology, Investigation, Validation, Writing-Original Draft, Writing-Review & Editing. **Zhengfang Liao:** Methodology, Investigation, Validation. **Xiaoqi Meng:**

Investigation, Formal Analysis. **A Erpuding · Ai Niwaer:** Validation. **Hongyue Wang:** Formal Analysis. **Xinhua Li:** Project Administration. **Deming Liu:** Conceptualization, Supervision, Project Administration, Writing-Review & Editing. **Fang Zuo:** Conceptualization, Supervision, Project Administration, Writing-Review & Editing, Resources.

# Graphic Abstract

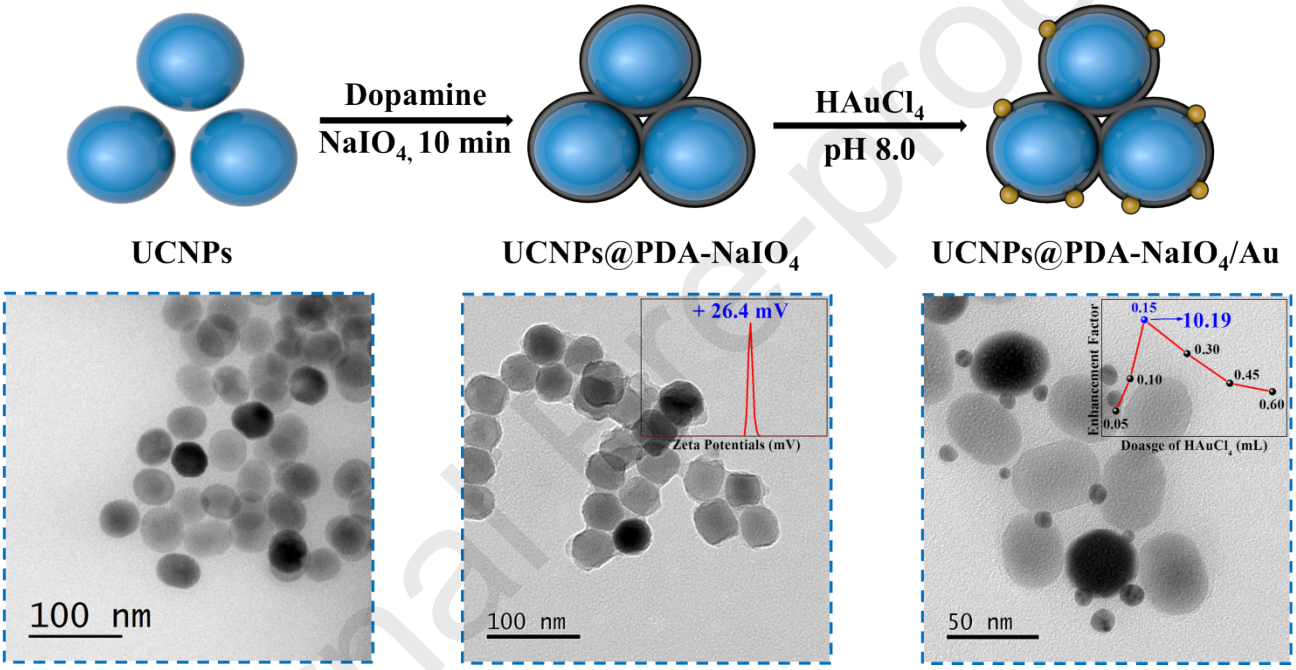


**Highlights**

- Hydrophobic UCNPs were fast coated by polydopamine (PDA) using $NaIO_4$ as an oxidant.
- PDA-coated UCNPs exhibit positive charge using $NaIO_4$ as an oxidant.
- Au nanoparticles (NPs) were deposited on PDA-coated UCNPs.
- pH can affect deposition of Au NPs on PDA coated UCNPs.
- Upconversion luminescence intensity could be regulated by the density of Au NPs.